Int J Clin Exp Med 2015;8(7):10956-10963
www.ijcem.com /ISSN:1940-5901/IJCEM0009254

Original Article

Acoustic radiation force impulse induced strain elastography and point shear wave elastography for evaluation of thyroid nodules

Xian Huang[1,2*], Le-Hang Guo[3,4*], Hui-Xiong Xu[3,4,5], Xue-Hao Gong[1,2], Bo-Ji Liu[3,4], Jun-Mei Xu[3,4], Yi-Feng Zhang[3,4], Xiao-Long Li[3,4], Dan-Dan Li[3,4], Shen Qu[4,6], Lin Fang[4,7]

[1]Department of Ultrasound, Shenzhen Second People's Hospital, First Hospital Affiliated to Shenzhen University, Shenzhen 518035, China; [2]Clinical School of Shenzhen Second People's Hospital, Anhui Medical University, Hefei 230032, China; Departments of [3]Medical Ultrasound, [6]Endocrinology and Metabolism, [7]Thyroid and Breast Surgery, Shanghai Tenth People's Hospital, Tongji University School of Medicine, Shanghai 200072, China; [4]Thyroid Institute, Tongji University School of Medicine, Shanghai 200072, China; [5]Department of Ultrasound, Guangdong Medical College Affiliated Hospital, Zhanjiang 524001, China. [*]Equal contributors.

Received April 17, 2015; Accepted June 15, 2015; Epub July 15, 2015; Published July 30, 2015

Abstract: The aim of the study was to evaluate the diagnostic performance of acoustic radiation force impulse (ARFI) induced strain elastography (SE), point shear wave elastography (p-SWE), and their combined use in differentiating thyroid nodules. This retrospective study included 155 thyroid nodules (94 benign and 61 malignant) in 136 patients. Ultrasound, ARFI-induced SE and p-SWE were performed on each nodule. Receiver operating characteristic curve (ROC) analyses were performed to assess the diagnostic efficacy of ARFI-induced SE, p-SWE and their combined use to distinguish benign from malignant thyroid nodules with histological results used as the reference standard. The areas under the ROC for ARFI-induced SE, p-SWE, and their combined use were 0.828, 0.829, and 0.840, respectively (both P > 0.05). The specificity of ARFI-induced SE was higher than that of p-SWE as well as their combined use (both $P < 0.05$). The combination of the two methods significantly improved the diagnostic sensitivity and NPV compared with either ARFI-induced SE or p-SWE alone (both $P < 0.05$). For nodules ≤ 10 mm, the combination of the two methods significantly improved the diagnostic sensitivity only. For nodules > 10 mm, there were no significant differences in sensitivity and NPV among the three methods in differentiating thyroid nodules (all $P > 0.05$). In conclusions, ARFI-induced SE and p-SWE are both valuable tools for detecting malignant thyroid nodules. The combined use of ARFI-induced SE and p-SWE improves the diagnostic sensitivity and NPV significantly whereas ARFI-induced SE alone achieves the highest specificity.

Keywords: Acoustic radiation force impulse induced strain elastography, point shear wave elastography, thyroid nodules

Introduction

The prevalence of thyroid nodules assessed by high frequency ultrasound (US) examination has increased to 68% in general population [1], and 14% of thyroid nodules were malignant [2]. US is the principal imaging method in identification of thyroid nodules. However, its diagnostic performance is unstable, which is highly depended on the experience and skills of the operators [3-6].

Hard thyroid nodules are more suspicious for malignancy [7]. Tissue stiffness can be evaluated by acoustic radiation force impulse (ARFI) elastography, a new imaging method that appeared in recent years. In this method, tissue is mechanically excited with short-duration acoustic pulses to generate localized tissue displacement. Localized tissue displacement is less in harder tissues than in softer ones. ARFI elastography included ARFI-induced strain elastography (SE) and point shear wave elastography (p-SWE). ARFI-induced SE estimates the tissue elasticity of the whole nodule qualitatively, by displaying the repetition of tissue displacement process along multiple image lines as a gray scale image, whereas p-SWE mea-

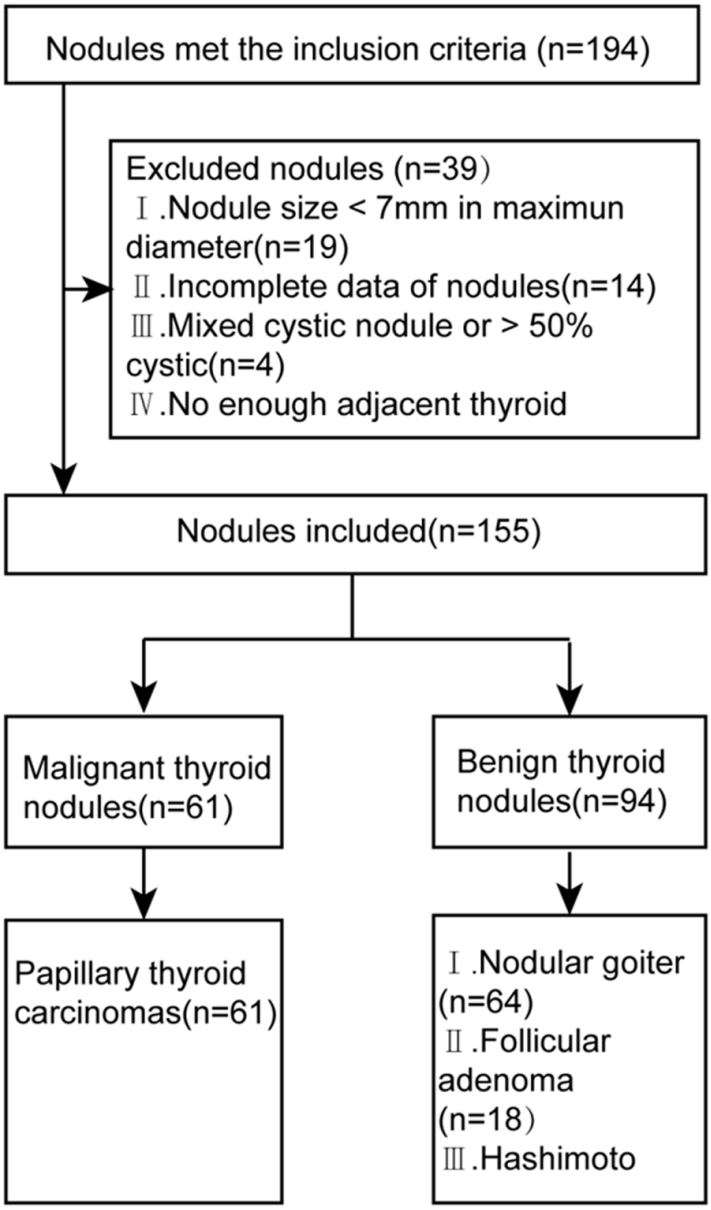

Figure 1. Flowchart of the selection of the thyroid nodules.

sures the elasticity in a selected region in the nodule quantitatively by calculating the shear wave velocity (SWV). A number of studies have affirmed the value of p-SWE in diagnosis of nodules [8-10]. However, only few studies have reported the diagnostic efficacy of ARFI-induced SE [11] and compared p-SWE and ARFI-induced SE in differentiating benign and malignant thyroid nodules [12, 13]. In addition, to our knowledge, no studies have shown the combined value of ARFI-induced SE and P-SWE. The aim of our study was to compare the diagnostic efficacy of ARFI-induced SE, p-SWE and their combined use in differentiating thyroid nodules.

Materials and methods

Patients

From November 2012 to March 2013, 155 nodules in 136 patients were included in this retrospective study. The institutional review board approved this study, and all involved patients provided informed consent to include the data for analysis. Inclusion criteria were as follows: (1) Nodules underwent US, p-SWE and ARFI-induced SE. (2) Nodules were confirmed by histopathology after surgery. Nodules with following criteria were excluded: (1) Maximum diameter of nodule was less than 7 mm. (2) Image data of nodules were not complete: US, p-SWE, or ARFI-induced SE image quality was poor. (3) Mixed cystic (< 50% solid) or almost cystic nodules. (4) There was no enough thyroid tissue surrounding the nodule. The flowchart for the selection of patients was presented in **Figure 1**.

The included patients consisted of 33 males and 103 females. The patient age was 51 ± 12 years (range, 22-78 years). Twenty-seven patients had one nodule and 109 had multiple nodules. The maximal diameter of the nodules was 16.9 ± 10.0 mm (range, 7-53 mm).

US, p-SWE, and ARFI-induced SE examinations

The US and ARFI examinations were performed using the S2000 US scanner (Siemens Medical Solutions, Mountain View, CA, USA) with a 4-9-MHz linear probe. All patients were scanned in the supine position with the neck slightly extended.

US images were obtained for each target nodule in both transverse and longitudinal planes. The target nodule was evaluated for size (largest diameter was 7-10 mm, or > 10 mm), loca-

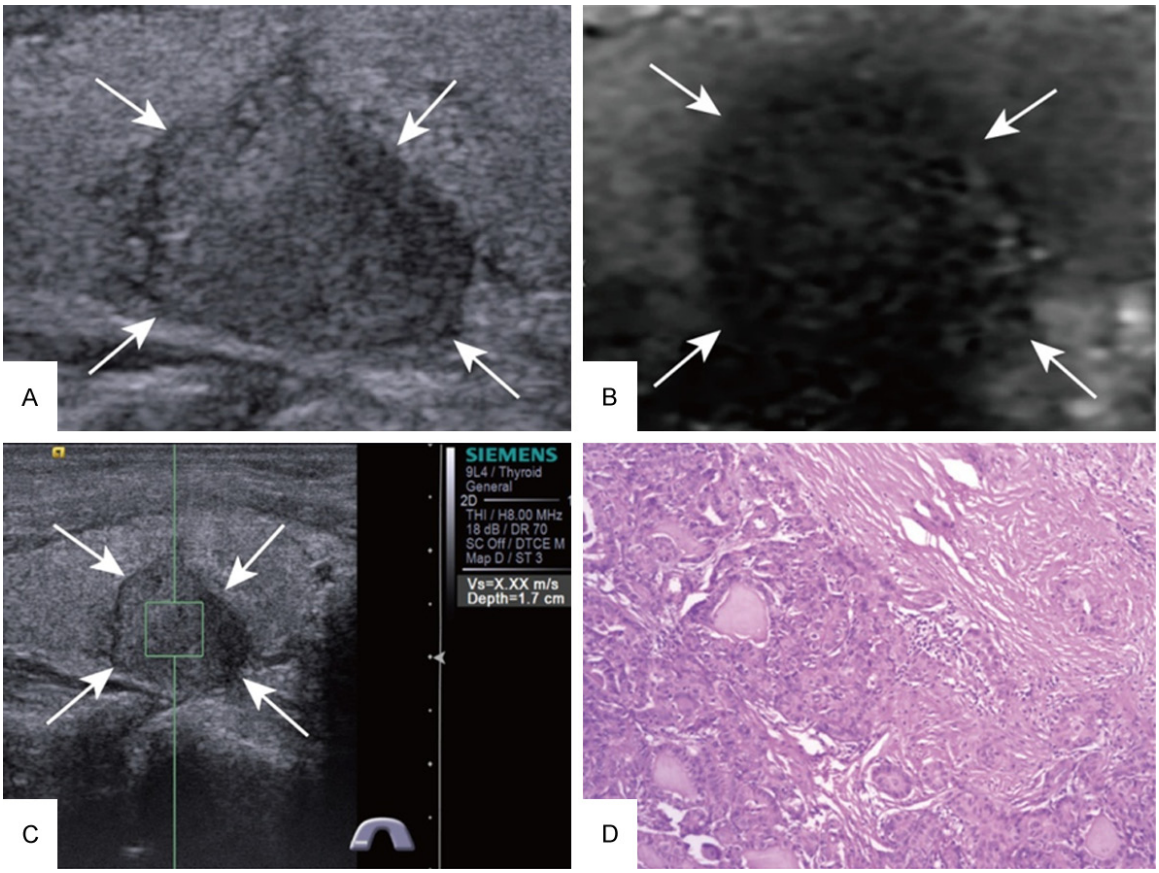

Figure 2. Images acquired in a 63-year-old woman. A. At conventional US, a 15-mm nodule appears solid in the right lobe of the thyroid. B. ARFI-induced SE score of 4. C. SWV of X.XX m/s on p-SWE. D. Histopathological examination of the thyroid nodule confirms the diagnosis of papillary carcinoma after surgery (Hematoxylin and eosin stain, × 100). US = ultrasound, ARFI = acoustic radiation force impulse, SE = strain elastography, SWV = shear wave velocity, p-SWE = point shear wave elastography.

tion (left lobe, right lobe, or isthmus), and internal components (solid or cystic).

ARFI-induced SE was performed following conventional US. The ARFI-induced SE image reflects the tissue elasticity with grayscale image in the field of view (FOV), in which the white indicates soft tissue whereas the black indicates hard tissue. To obtain qualified images, patients were asked to hold their breath. The probe was placed on the body surface with light pressure, and FOV was adjusted to include the whole nodule and some surrounding thyroid tissue. Tissue stiffness on ARFI-induced SE was scored from 1 (soft) to 6 (hard), according to Xu's scoring system [11]: 1, predominantly white; 2, predominantly white with a small amount of black; 3, equally white and black; 4, predominantly black with a few white spots; 5, almost completely black; and 6, completely black without white spots. Based on the previous study, grade ≥ 4 was considered for malignancy [11].

p-SWE reflects the stiffness of tissue quantitatively with the SWV (m/s). The region of interest (ROI) was placed on the solid portion of the nodule, avoiding bulky calcification and fluid portion as far as possible during measurement. The measurement was repeated for seven times without movement of the probe. The maximum and minimum values of the seven measurements were excluded, and the mean of the remaining values was calculated and used for analysis. Nodule measurement expressed as X.XX m/s was occasionally found. Several possible explanations for the phenomenon were as follows: patient's respiration or motion, operator's inappropriate gesture, and measurements of fluid portion or tissue stiffness beyond the p-SWE measuring range (0.5-8.4 m/s). After excluding other possible expla-

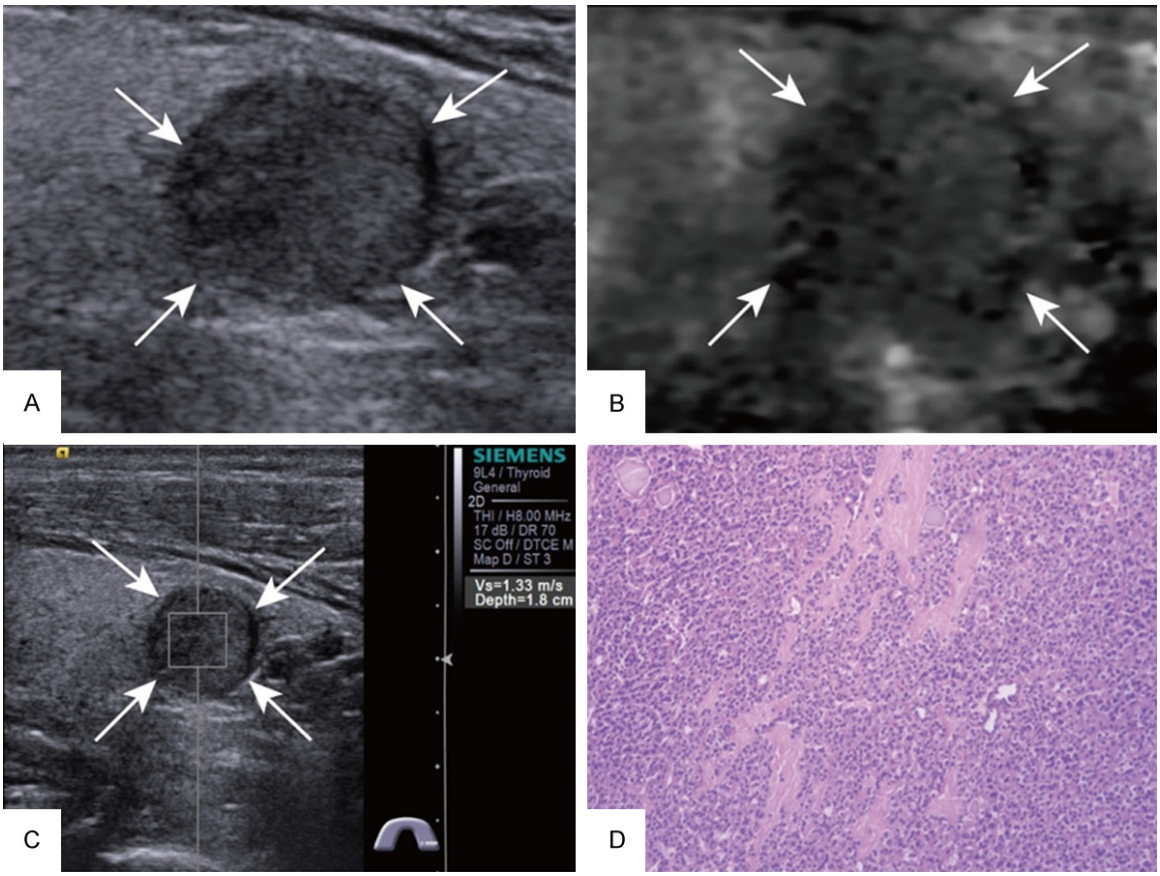

Figure 3. Images acquired in a 60-year-old man. A. At conventional US, a 12-mm nodule appears solid in the left lobe of the thyroid. B. ARFI-induced SE score of 3. C. SWV of 1.33 m/s on p-SWE. D. Histopathological examination of the thyroid nodule confirms the diagnosis of follicular adenoma after surgery (Hematoxylin and eosin stain, × 100). US = ultrasound, ARFI = acoustic radiation force impulse, SE = strain elastography, SWV = shear wave velocity, p-SWE = point shear wave elastography.

nations, the measurement result of "X.XX m/s" was replaced by 8.4 m/s, because all the nodules included in our study were solid or > 50% solid.

Statistics analysis

Statistical analyses were performed by using SPSS software version 19.0 (SPSS Inc, Chicago, IL, USA). $P < 0.05$ was considered to be statistically significant. Continuous variables were analyzed by the independent t test. Receiver-operating characteristic (ROC) curve analyses were performed to assess the diagnostic performance of the three methods in differentiating benign from malignant thyroid nodules. The comparison of areas under the ROC curve (AUCs) was performed by Z test. The best cut-off value of SWV was obtained when Youden index (YI) was maximum. The sensitivity, specificity, accuracy, positive predictive values (PPV), negative predictive values (NPV), and YI of p-SWE, ARFI-induced SE and their combined use for differentiating thyroid nodules were calculated comparing the findings with histological results. Differences in sensitivity, specificity, and accuracy were tested using the McNemar test and that in PPV and NPV were tested by chi-square test.

Results

Histopathological analysis

Of the 155 thyroid nodules, 61 were malignant (**Figure 2** is an example of a malignant nodule) and 94 were benign (**Figure 3** is an example of a benign nodule). All of the malignant nodules were papillary carcinomas. In the group of benign nodules, the diagnosis included nodular goiter (n = 64), adenoma (n = 18), and Hashimoto's nodule (n = 12).

Table 1. Characteristics of the patients and the nodules

Characteristic	Benign	Malignant
Patients*	81	55
Age (years)	54 ± 11 (25-77)	47 ± 13 (22-78)
Gender		
Female	59	44
Male	22	11
Nodules	94	61
Size (mm)	20.4 ± 10.9 (7-53)	21.1 ± 10.8 (7-28)
7-10 mm	21	37
> 10 mm	73	24
Location		
Left lobe	49	23
Right lobe	40	34
Isthmus	5	4

Note-*Patients with multiple nodules were classified into malignant group, when they had at least one nodule that was histopathological proved malignant.

Table 2. Histopathologic Types and SE Scores for the Thyroid Nodules

Histopathology results	ARFI-induced SE score						
	1	2	3	4	5	6	Total
Benign nodules (n = 100)							
Nodular goiter	2	23	33	5	1	0	64
Adenoma	0	10	6	1	0	1	18
Hashimoto nodule	0	2	9	1	0	0	12
Total	2	35	48	7	1	1	94
Malignant nodules (n = 72)							
Papillary carcinoma	0	6	10	35	10	0	61

Note-ARFI = acoustic radiation force impulse, SE = strain elastography.

Characteristics of patients and nodules

The basic characteristics of the patients and the nodules are presented in **Table 1**. In patients with multiple nodules, 1 nodule in each patient from 91 patients (including 58 benign and 33 malignant nodules), 2 nodules in each patient from 17 patients (including 6 with 2 benign nodules in each, 4 with 2 malignant nodules in each, and 7 with 1 benign and 1 malignant nodule), 3 nodules in each from 1 patients (including 2 malignant and 1 benign nodules) were included in this study.

The ARFI characteristics of the thyroid nodules

ARFI-induced SE scores of thyroid nodules with different pathology types are presented in **Table 2**. The mean SWV of 94 benign thyroid nodules was 2.32 ± 1.08 m/s (range, 0.36-7.20 m/s), and the mean SWV of 61 malignant thyroid nodules was 4.40 ± 2.31 m/s (range, 1.52-8.40 m/s) ($P < 0.001$). ROC curve analyses showed that the best SWV cutoff value was 2.64 m/s. When ARFI-induced SE and p-SWE were combined, the nodule was considered malignant as long as meeting one of the following two conditions: first, ARFI-induced SE score was 4 or above; second, SWV ≥ 2.64 m/s.

Diagnostic performance of the three methods

The sensitivity, specificity, accuracy, PPV, NPV, YI and AUC of the three methods are presented in **Table 3**. The specificity of ARFI-induced SE was higher than that of p-SWE as well as their combined use (both $P < 0.05$). The sensitivity and NPV were increased by the use of a combination of ARFI-induced SE and p-SWE in comparison with ARFI-induced SE or p-SWE alone (both $P < 0.05$). There were no significant differences in accuracy, PPV and AUC among the three modalities (all $P > 0.05$).

When dividing the nodules into two groups with different sizes, for the nodules ≤ 10 mm, the best SWV cutoff value of p-SWE was 3.21 m/s. The sensitivity of the combined use was higher than that of ARFI-induced SE or p-SWE alone (both $P < 0.05$), and there were no significant differences in accuracy, PPV, NPV and AUC among the three modalities (all $P > 0.05$). On the other hand, the best SWV cutoff value of p-SWE was 2.64 m/s for the nodules > 10 mm. Only the specificity of ARFI-induced SE was higher than that of the combined use ($P < 0.05$). The diagnostic performance results of the three methods in groups with different sizes are summarized in **Table 3**.

Discussion

Most of thyroid nodules are benign, whereas the risk of malignancy cannot be neglected. Fine-needle aspiration biopsy (FNA) is the most accurate and cost-effective method to distinguish benign thyroid nodules from those at risk for malignancy [14]. With the development of the US technology, many thyroid nodules are detected without clinical symptoms, and the decision to perform FNA mainly depended on the US characteristics of the nodules. In addi-

Table 3. Performance of ARFI-induced SE, p-SWE, and their combined use in differentiating benign from malignant lesions in different size

Groups		Sensitivity (%)	Specificity (%)	Accuracy (%)	PPV (%)	NPV (%)	YI	AUC
≤ 10 mm	ARFI-induced SE	64.9 (24/37)	81.0 (17/21)	70.7 (41/58)	85.7 (24/28)	56.7 (17/30)	0.458	0.704
	p-SWE	59.5 (22/37)	85.7 (18/21)	69 (40/58)	88 (22/25)	54.5 (18/33)	0.452	0.773
	ARFI-induced SE/p-SWE	89.2[a] (33/37)	61.9 (13/21)	79.3 (46/58)	80.5 (33/41)	76.5 (13/17)	0.511	0.755
> 10 mm	ARFI-induced SE	87.5 (21/24)	93.2[b] (68/73)	91.8 (89/97)	80.8 (21/26)	95.8 (68/71)	0.807	0.912
	p-SWE	83.3 (20/24)	82.2 (60/73)	82.5 (80/97)	60.6 (20/33)	93.8 (60/64)	0.655	0.844
	ARFI-induced SE/p-SWE	100 (24/24)	78.1 (57/73)	81.4 (79/97)	60.0 (24/40)	100 (57/57)	0.781	0.89
Total	ARFI-induced SE	73.8 (45/61)	90.4[d] (85/94)	83.9 (130/155)	83.3 (45/54)	84.2 (85/101)	0.642	0.828
	p-SWE	82 (50/61)	76.6 (72/94)	78.7 (122/155)	69.4 (50/72)	86.7 (72/83)	0.569	0.829
	ARFI-induced SE/p-SWE	96.7[c] (59/61)	71.2 (67/94)	81.3 (125/155)	68.6 (59/86)	97.1[e] (67/69)	0.68	0.84

Note-[a]Compared with sensitivity of ARFI-induced SE and p-SWE in nodules ≤ 10 mm, both $P < 0.05$. [b]Compared with specificity of ARFI-induced SE/p-SWE only in nodules > 10 mm, $P < 0.01$. [c]Compared with sensitivity of ARFI-induced SE and p-SWE in all nodules, both $P < 0.01$. [d]Compared with specificity of p-SWE and ARFI-induced SE/p-SWE in all nodules, both $P < 0.05$. [e]Compared with NPV of ARFI-induced SE and p-SWE in all nodules, both $P < 0.05$. ARFI = acoustic radiation force impulse, SE = strain elastography, p-SWE = point shear wave elastography. PPV = positive predictive values, NPV = negative predictive values, YI = Youden index, AUC = area under the receiver-operating characteristic curve.

tion, the incidence of differentiated thyroid cancer of all sizes has been increasing in recent years [15]. Therefore, US tools with a high sensitivity for malignancy are needed to minimize the risk of missing malignant nodules not submitted to FNA.

The technique p-SWE could provide quantitative elasticity information for tissue, with a sensitivity range of 71.6-100%, a specificity range of 75-95.7%, an accuracy range of 80.3-96.13%, a PPV range of 58.9-93.75%, and a NPV range of 90-97.8% in the differential diagnosis between malignant and benign thyroid nodules [8, 10, 16-19]. In addition, Zhang et al [18] reported a reasonable intraobserver and interobserver reproducibility of p-SWE. In our study, the sensitivity, specificity, accuracy, PPV and NPV were 82%, 76.6%, 78.7%, 69.4%, and 86.7%, respectively, when using a cut-off value of 2.64 m/s. These are equivalent or slightly lower than those in previous studies. The reason was most likely because 37.4% (58/155) of nodules in our study were small (≤ 10 mm). For nodules ≤ 10 mm, calcification is difficult to exclude, as the ROI has a fixed size of 6 × 5 mm, which eventually leads to a higher p-SWE value. For ARFI-induced SE, Zhang et al [11] found that the sensitivity, specificity, accuracy, PPV and NPV were 87.0%, 95.8%, 92.7%, 91.8%, and 93.1%, respectively. In our study, the sensitivity, specificity, accuracy, PPV and NPV were 73.8%, 90.4%, 83.9%, 83.3% and 84.2%, respectively. The sensitivity of p-SWE and ARFI-induced SE were not high enough (82% and 73.8%). When the two methods were combined, the sensitivity increased to 96.7% and NPV increased to 97.1% at the same time, yet the specificity reduced to 71.2%. Further studies should evaluate whether the results are suitable to the following situations as well, such as thyroid nodules in high risk groups [14] or nodules with suspicious US features were diagnosed as benign by FNA.

Papillary thyroid carcinoma (PTC) is the most common thyroid malignancy, the major task of modern imaging techniques is to make a differentiation between it and benign nodules. PTC can be defined as a thyroid papillary microcarcinoma (PTMC) when it is less than 10 mm. The incidence of lymph node metastasis in PTMC ranges from 24% to 64% [20-23]. Routine FNA is not recommended for nodules < 1 cm, unless the following problems were existing: suspicious US findings of nodules and abnormal lymph nodes, family history of papillary thyroid carcinoma, history of irradiation as a child, history of hemithyroidectomy with discovery of thyroid cancer before and so on. Furthermore, FNA has a high inadequate specimen rate. The diagnosis of PTMC was difficult compared with the cancer > 1 cm. A previous study [24] showed that ARFI elastography seems to be a valuable tool for the differential diagnosis of thyroid nodules ≤ 1 cm, in which, the sensitivity, specificity, and accuracy were 61.4%, 88.3%, and 73.4%, respectively for ARFI-induced SE; 56.2%, 79.2%, and 66.5% for p-SWE, in consistent with those in our study. In summary, the sensitivity of ARFI for the diagnosis of malignancy in thyroid nodules ≤ 10 mm is low. With regard to combined use of p-SWE and ARFI-induced SE, the sensitivity obviously improved. Thus, the rate of missed diagnosis could be reduced. For the nodules > 10 mm, there was

no difference of sensitivity, accuracy, PPV, and NPV among p-SWE, ARFI-induced SE, and their combined use in differentiating thyroid nodules.

There were several limitations in our study. First, this was a retrospective study with a limited sample size and all of the malignancies were papillary thyroid carcinomas; second, nodules with diameters less than 7 mm were excluded from the study, because ROI was fixed at 6 × 5 mm, ARFI could not give reliable information about the tissue stiffness. Thus, further studies with more sample size and varied tumor types are required to validate the study results.

In conclusions, p-SWE and ARFI-induced SE have been shown potent value in the characterization of thyroid nodules between the benign and malignant nodules. The combined use of p-SWE and ARFI-induced SE improves the diagnostic sensitivity and NPV significantly whereas ARFI-induced SE alone achieves the highest specificity, which is relevant in clinical practice.

Acknowledgements

This work was supported in part by Grant SHDC12014229 from Shanghai Hospital Development Center and Grant 2012045 from Shanghai Human Resource and Social Security Bureau, Grant 81401417 from the National Natural Science Foundation of China and Grant JCYJ20140414170821285 from Shenzhen science and technology innovation committee.

Disclosure of conflict of interest

None.

Address correspondence to: Hui-Xiong Xu, Department of Medical Ultrasound, Shanghai Tenth People's Hospital, Tenth People's Hospital of Tongji University, Shanghai 200072, China. E-mail: xuhuixiong@hotmail.com; Xue-Hao Gong, Department of Ultrasound, Shenzhen Second People's Hospital, First Hospital Affiliated to Shenzhen University, Shenzhen 518035, China. E-mail: fox_gxh@sina.com

References

[1] Guth S, Theune U, Aberle J, Galach A and Bamberger CM. Very high prevalence of thyroid nodules detected by high frequency (13 MHz) ultrasound examination. Eur J Clin Invest 2009; 39: 699-706.

[2] Yassa L, Cibas ES, Benson CB, Frates MC, Doubilet PM, Gawande AA, Moore FD Jr, Kim BW, Nose V, Marqusee E, Larsen PR and Alexander EK. Long-term assessment of a multidisciplinary approach to thyroid nodule diagnostic evaluation. Cancer 2007; 111: 508-516.

[3] Cooper DS, Doherty GM, Haugen BR, Kloos RT, Lee SL, Mandel SJ, Mazzaferri EL, McIver B, Sherman SI and Tuttle RM. Management guidelines for patients with thyroid nodules and differentiated thyroid cancer. Thyroid 2006; 16: 109-142.

[4] Sipos JA. Advances in ultrasound for the diagnosis and management of thyroid cancer. Thyroid 2009; 19: 1363-1372.

[5] Moon HJ, Sung JM, Kim EK, Yoon JH, Youk JH and Kwak JY. Diagnostic performance of gray-scale US and elastography in solid thyroid nodules. Radiology 2012; 262: 1002-1013.

[6] Unluturk U, Erdogan MF, Demir O, Gullu S and Baskal N. Ultrasound elastography is not superior to grayscale ultrasound in predicting malignancy in thyroid nodules. Thyroid 2012; 22: 1031-1038.

[7] Sun J, Cai J and Wang X. Real-time ultrasound elastography for differentiation of benign and malignant thyroid nodules: a meta-analysis. J Ultrasound Med 2014; 33: 495-502.

[8] Grazhdani H, Cantisani V, Lodise P, Di RG, Proietto MC, Fioravanti E, Rubini A and Redler A. Prospective evaluation of acoustic radiation force impulse technology in the differentiation of thyroid nodules: accuracy and interobserver variability assessment. J Ultrasound 2014; 17: 13-20.

[9] Zhan J, Diao XH, Chai QL and Chen Y. Comparative study of acoustic radiation force impulse imaging with real-time elastography in differential diagnosis of thyroid nodules. Ultrasound Med Biol 2013; 39: 2217-2225.

[10] Zhang FJ and Han RL. The value of acoustic radiation force impulse (ARFI) in the differential diagnosis of thyroid nodules. Eur J Radiol 2013; 82: e686-690.

[11] Zhang YF, He Y, Xu HX, Xu XH, Liu C, Guo LH, Liu LN and Xu JM. Virtual touch tissue imaging on acoustic radiation force impulse elastography: a new technique for differential diagnosis between benign and malignant thyroid nodules. J Ultrasound Med 2014; 33: 585-595.

[12] Zhang FJ, Han RL and Zhao XM. The value of virtual touch tissue image (VTI) and virtual touch tissue quantification (VTQ) in the differential diagnosis of thyroid nodules. Eur J Radiol 2014; 83: 2033-2040.

[13] Gu J, Du L, Bai M, Chen H, Jia X, Zhao J and Zhang X. Preliminary study on the diagnostic value of acoustic radiation force impulse technology for differentiating between benign and

malignant thyroid nodules. J Ultrasound Med 2012; 31: 763-771.
[14] Cooper DS, Doherty GM, Haugen BR, Kloos RT, Lee SL, Mandel SJ, Mazzaferri EL, McIver B, Pacini F, Schlumberger M, Sherman SI, Steward DL and Tuttle RM. Revised American Thyroid Association management guidelines for patients with thyroid nodules and differentiated thyroid cancer. Thyroid 2009; 19: 1167-1214.
[15] Chen AY, Jemal A and Ward EM. Increasing incidence of differentiated thyroid cancer in the United States, 1988-2005. Cancer 2009; 115: 3801-3807.
[16] Hamidi C, Goya C, Hattapoglu S, Uslukaya O, Teke M, Durmaz MS, Yavuz MS, Hamidi A and Tekbas G. Acoustic Radiation Force Impulse (ARFI) imaging for the distinction between benign and malignant thyroid nodules. Radiol Med 2015; 120: 579-83.
[17] Deng J, Zhou P, Tian SM, Zhang L, Li JL and Qian Y. Comparison of diagnostic efficacy of contrast-enhanced ultrasound, acoustic radiation force impulse imaging, and their combined use in differentiating focal solid thyroid nodules. PLoS One 2014; 9: e90674.
[18] Zhang YF, Xu HX, He Y, Liu C, Guo LH, Liu LN and Xu JM. Virtual touch tissue quantification of acoustic radiation force impulse: a new ultrasound elastic imaging in the diagnosis of thyroid nodules. PLoS One 2012; 7: e49094.
[19] Xu JM, Xu XH, Xu HX, Zhang YF, Zhang J, Guo LH, Liu LN, Liu C and Zheng SG. Conventional US, US elasticity imaging, and acoustic radiation force impulse imaging for prediction of malignancy in thyroid nodules. Radiology 2014; 272: 577-586.
[20] Wada N, Duh QY, Sugino K, Iwasaki H, Kameyama K, Mimura T, Ito K, Takami H and Takanashi Y. Lymph node metastasis from 259 papillary thyroid microcarcinomas: frequency, pattern of occurrence and recurrence, and optimal strategy for neck dissection. Ann Surg 2003; 237: 399-407.
[21] Chow SM, Law SC, Chan JK, Au SK, Yau S and Lau WH. Papillary microcarcinoma of the thyroid-Prognostic significance of lymph node metastasis and multifocality. Cancer 2003; 98: 31-40.
[22] Hay ID, Hutchinson ME, Gonzalez-Losada T, McIver B, Reinalda ME, Grant CS, Thompson GB, Sebo TJ and Goellner JR. Papillary thyroid microcarcinoma: a study of 900 cases observed in a 60-year period. Surgery 2008; 144: 980-987; discussion 987-988.
[23] So YK, Son YI, Hong SD, Seo MY, Baek CH, Jeong HS and Chung MK. Subclinical lymph node metastasis in papillary thyroid microcarcinoma: a study of 551 resections. Surgery 2010; 148: 526-531.
[24] Zhang YF, Liu C, Xu HX, Xu JM, Zhang J, Guo LH, Zheng SG, Liu LN and Xu XH. Acoustic radiation force impulse imaging: a new tool for the diagnosis of papillary thyroid microcarcinoma. Biomed Res Int 2014; 2014: 416969.